We are IntechOpen,
the world's leading publisher of
Open Access books
Built by scientists, for scientists

6,100
Open access books available

167,000
International authors and editors

185M
Downloads

154
Countries delivered to

Our authors are among the

TOP 1%
most cited scientists

12.2%
Contributors from top 500 universities

CLARIVATE ANALYTICS
BOOK CITATION INDEX
INDEXED

WEB OF SCIENCE™

Selection of our books indexed in the Book Citation Index
in Web of Science™ Core Collection (BKCI)

Interested in publishing with us?
Contact book.department@intechopen.com

Chapter

Spaceborne Video Synthetic Aperture Radar (SAR): A New Microwave Remote Sensing Mode

Jian Liang and Liang An

Abstract

The transient information like a 'picture' can be obtained by the traditional microwave remote sensing system. It will bring some shortcomings for detection of the moving targets and long-time monitoring of the variational scene over the region of interest. As a new imaging mode, more and more scholars and agencies have focused on the video Synthetic Aperture Radar (SAR) due to it can provide continuous surveillance over the region of interest. The spaceborne video SAR has the corresponding advantages over the spaceborne SAR image system and the optical video system. The working principles, imaging algorithm, and application method of spaceborne video SAR have been proposed in this chapter. First of all, a theoretical System of spaceborne video SAR has been constructed. The operation and application mode have also been defined. Some key performances have been discussed. To meet the demand for video SAR applications, one imaging algorithm has been proposed for dealing with the spaceborne video SAR data. Experiments on simulated data show that the algorithm was effective.

Keywords: video SAR, working principles, imaging algorithm, moving target detection, parameter estimation

1. Introduction

Video SAR (synthetic aperture radar) is a new imaging mode that can provide continuous surveillance over a region of interest [1]. Compared with traditional SAR imaging, the SAR image stream of spaceborne video SAR is acquired by rapid imaging in a short time. Due to its dynamic information acquisition ability, video SAR is more suitable for the observation of moving targets and time-varying scenes [2–8]. The main work and contributions of this chapter are summarized as follows.

1. A theoretical system of spaceborne video SAR has been constructed. Based on the traditional spaceborne SAR system, the concept of spaceborne video SAR was introduced. The operation and application mode have also been defined. Some key performances, such as resolution, duration of the different operation times, and division method of the raw data have been discussed.

2. To meet the demand for video SAR applications, such as high accuracy and efficient computation. One imaging algorithm has been proposed for dealing with the spaceborne video SAR data. The image formation algorithms can avoid the duplication of processing, to improve the computation efficiency. Finally, experiments on simulated data show that the proposed algorithms were effective.

This chapter has broken through some key technologies in the construction and application of spaceborne video SAR system. The research result can be used as advice to build a spaceborne video SAR system.

2. The theory of spaceborne video SAR

2.1 SAR imaging

Synthetic aperture radar is a two-dimensional high-resolution imaging radar, whose high resolution in the range direction is achieved by transmitting LFM signal followed by matched filtering. The azimuth high resolution is achieved by using the relative motion between the radar and the target to form an equivalent large aperture [9, 10].

2.2 Spaceborne video SAR

Broadly speaking, video is generally defined as a number of linked images played continuously at a certain frequency, which forms a moving image.

Narrowly defined video is generally used in movies or television, and refers to continuous image changes of more than 24 frames per second, according to the principle of visual transient, the human eye cannot distinguish a single static picture, looks like a smooth continuous visual effect, such a continuous picture is also called video.

The U.S. Defense Advanced Research Projects Agency (DARPA) has made a preliminary definition of video SAR: the technology that can reflect a series of SAR images of continuous changes of a target or scene displayed at a fixed frame rate is called video SAR [6].

2.2.1 The operating mode of spaceborne video SAR

In the application of spaceborne video SAR, multiple SAR imaging of the same scene is mainly realized, while the effective observation time is increased as much as possible. For airborne platforms, circular-track SAR is generally used to realize long-time observation of the scene, while for spaceborne platforms, the observation time can be effectively extended through reasonable orbit design to realize video observation.

1. GEO Video SAR

GEO SAR satellites can form a near-circular satellite trajectory to the earth through orbit design, providing the possibility of GEO circular-track video SAR, which can effectively extend the observation time while realizing the gaze on fixed scenes.
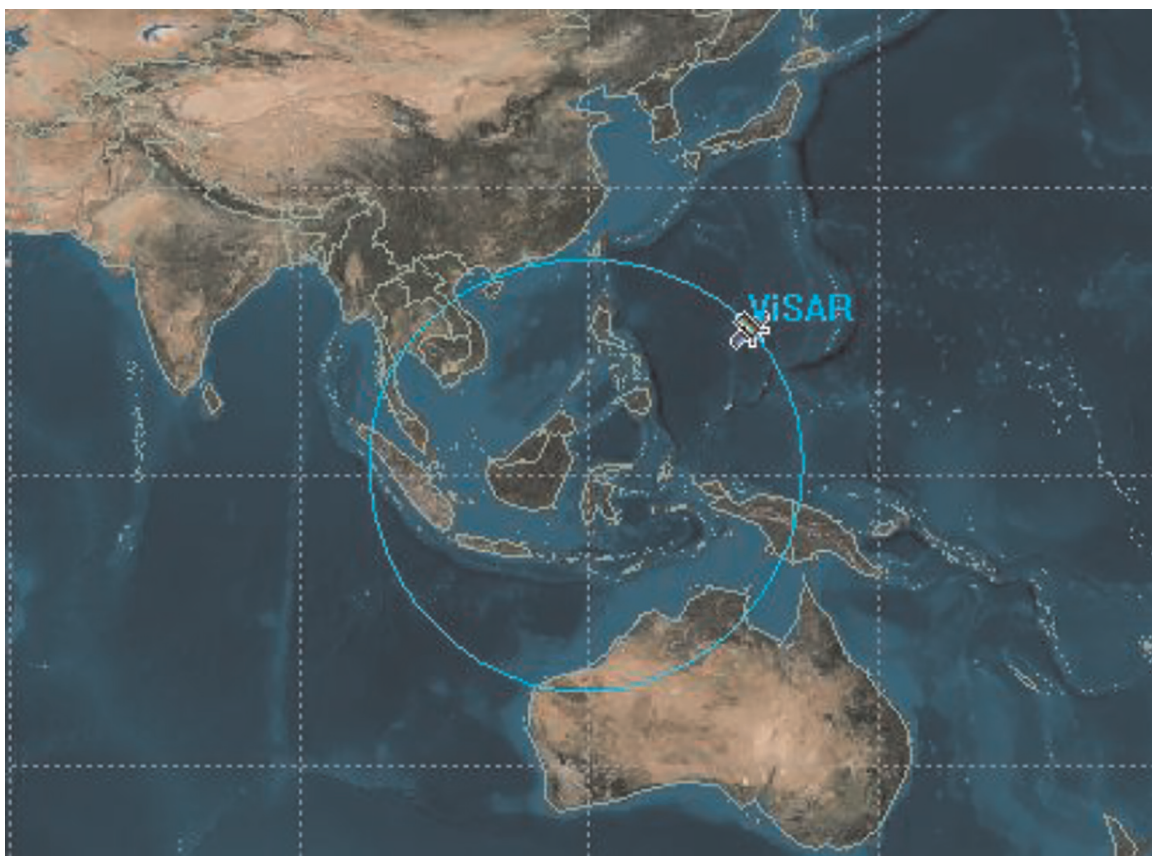
Figure 1.
GEOSAR satellite circular trajectory video SAR subsatellite point.

For geosynchronous orbit satellites, circular-track SAR for video imaging can be achieved by making the sub-satellite point trajectory circular. The design method is to control the north–south drift of the satellite to be equal to the east–west drift, the north–south drift is determined by the orbit inclination, while the east–west drift is determined by the eccentricity, and the ascending node determines the longitude of the circle track center. Thus, the circle-trace video observation can be realized by a reasonable orbit design. The sub-satellite point trajectory in the process of GEO circular-track video observation was shown in **Figure 1**.

2. Spotlight video SAR

To prolong the video SAR imaging time, the low-orbit satellite video SAR can work in the large-angle staring spotlight mode, in which the satellite uses the azimuth direction large-angle sweep capability to achieve a long time observation of the observation scene, and the conventional spotlight SAR improves the azimuthal resolution by extending the observation time, while the video SAR can achieve multiple imaging by reducing the azimuth resolution of a single image frame. Video imaging can be achieved by reasonably segmenting the echo data throughout the imaging time, and the geometric schematic of its imaging mode was shown in **Figure 2**.

3. Sliding spotlight video SAR

In order to increase the azimuthal width of the video imaging scene, the video SAR can also operate in sliding spotlight SAR, and the geometric schematic of its imaging

mode was shown in **Figure 3**, in which the satellite uses its agile maneuvering capability to perform sliding beam imaging of the observed scene, and then performs attitude maneuvering after the first image is completed to complete the second frame of video imaging, and repeats the imaging until it is beyond the satellite's attitude maneuvering capability or observable range, thus forming a video SAR image.

2.2.2 The applications of spaceborne video SAR

The spaceborne video SAR is actually a sequence of SAR images of the same target area with high update frequency, and the applications based on video SAR images mainly include the following aspects [11–13].

1. Multi-aspect observation of target

For the spaceborne video SAR, different video frames have different observation aspects of the target, so different video frames can achieve multi-aspect observation of
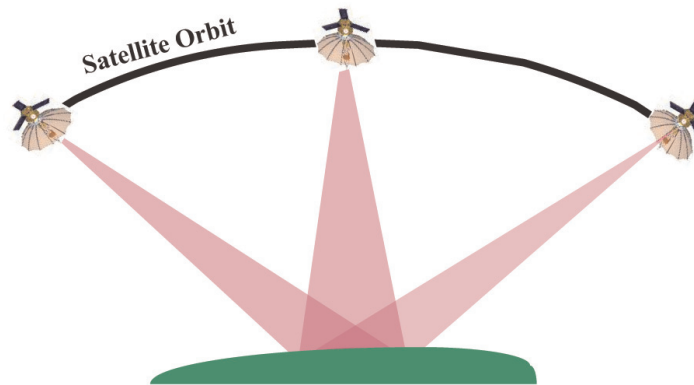

Figure 2.
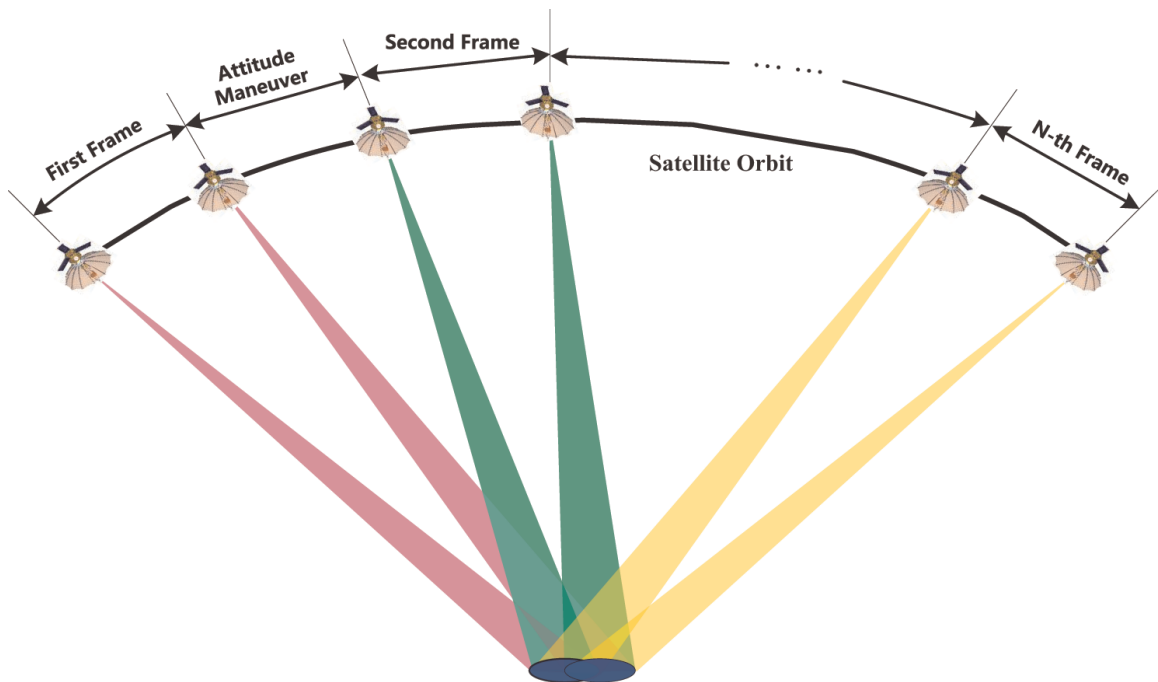*The geometric schematic of spotlight video SAR.*

Figure 3.
The geometric schematic of sliding spotlight video SAR.

the target, and the SAR images of the target under different observation aspects can fully describe the characteristic information of the target, which is of great significance to the target identification and confirmation.

2. Suppressing the coherent speckle of SAR images.

Coherence speckle refers to the subechoes of multiple scattering points superimposed or eliminated with the same phase in certain resolution units, which makes dotted bright or dark areas appear in SAR images. The traditional coherent speckle suppression method uses multi-look processing to achieve the non-coherent superposition of multi-look images. The effective suppression of coherent speckle can also be achieved in video SAR products by non-coherent superposition of multi-frame images.

3. Continuous monitoring of scenarios and targets [14–18]

The existing SAR moving target detection technology does not achieve continuous video monitoring of hotspot areas, and the ATI or DPCA-based moving target detection has the problems of minimum detection speed and blind speed, and the estimation of target motion parameters also has the problem of ambiguity, which brings greater challenges to the localization and imaging of moving targets. Video SAR effectively extends the information in the time dimension, and the detection of moving targets and estimation of motion parameters can be achieved by using the change information between frames. The video SAR products after locating and imaging moving targets can intuitively display the motion information such as position, velocity, and motion trend of moving targets in stationary scenes.

2.2.3 Analysis of imaging duration of spaceborne video SAR

The imaging duration of the spaceborne video SAR is mainly constrained by the following factors, and the minimum value of the video imaging duration determined by these factors is the imaging duration of the spaceborne video SAR.

1. Incidence angle constraint

The variation of the incidence angle affects the ground range resolution, and the incidence angle also affects the radar observation distance. In general, the backscattering cross section decreases with the increase of the incidence angle. From the perspective of energy return, the incidence angle should be chosen as small as possible within the applicable range of scattering theory, but from the perspective of application requirements, different application requirements require different incidence angles. The difficulty of system implementation will increase after the incidence angle is extended. Considering these factors, the constraint of incidence angle needs to be satisfied in the process of spaceborne video SAR imaging.

2. The beam azimuth sweeping capability constraint

The imaging duration of spaceborne video SAR is also constrained by the beam sweeping capability of the satellite. For phased-array antennas, the antenna gain decreases seriously during the large-angle sweeping process, and the dispersion effect will occur at the same time, resulting in the degradation of imaging quality, while the reflector antenna has the characteristics of stable antenna pattern and high gain

during the large-angle sweeping process. For the reflector antenna, the azimuth sweeping capability is mainly limited by the maneuverability of the agile platform. The sweeping capability determines the duration of the video imaging, and the larger the sweeping angle, the longer the video imaging time within the incidence angle meets the observation requirements.

3. Squint angle constraint

The coupling between range and azimuth direction is serious in the process of SAR imaging processing when the squint angle is large, which brings difficulties to the imaging processing, and the existing imaging processing algorithm has the maximum squint angle limitation if a good focusing effect is to be achieved. Therefore, the requirement of squint angle during imaging processing is also one of the constraints on the duration of video SAR imaging.

3. Image formation algorithm of spaceborne video SAR

The main two modes of video SAR implementation by LEO satellites are spotlight and sliding spotlight. Since there is no overlap of data between adjacent frames in sliding spotlight mode, the imaging algorithm in this mode is the same as the traditional imaging algorithm in sliding spotlight mode. In contrast, for the spotlight mode, there is overlap between adjacent video frames, and to avoid repeated operations of overlapping data, the imaging algorithm applicable to spaceborne video SAR needs to be studied. In this section, a video SAR imaging algorithm is proposed for the key technical problems to be solved in the process of video SAR imaging, and the simulation is verified.

3.1 Echo data segmentation method

Typically, the spaceborne radar is operated in the spotlight mode for an extended period of time while taking video. The conventional spotlight SAR imaging mode achieves the high azimuth resolution through lengthening the synthetic time, while in the video mode the spotlight raw data was divided into pieces to form the video frames. The image geometrical mode of spaceborne video SAR based on equivalent squint range mode was shown in **Figure 4**, in which L_s is the distance the radar moves throughout the video imaging progress. β is the largest synthetic angle, l_s is the distance the radar moves of a video frame. θ_i is the synthetic angle of a video frame, while θ_{ci} is the squint angle of the video frame. The equivalent velocity of the radar is v_r.

The Doppler bandwidth of the ith video frame can be expressed as follows.

$$Ba_i = fd_b - fd_a \tag{1}$$

Where fd_a and fd_b are the Doppler frequency at the start and end time of the ith video frame.

$$fd_a = -\frac{2v_r \cos\left(\theta_{ci} - \frac{\theta_i}{2}\right)}{\lambda} \tag{2}$$

$$fd_b = -\frac{2v_r \cos\left(\theta_{ci} + \frac{\theta_i}{2}\right)}{\lambda} \tag{3}$$
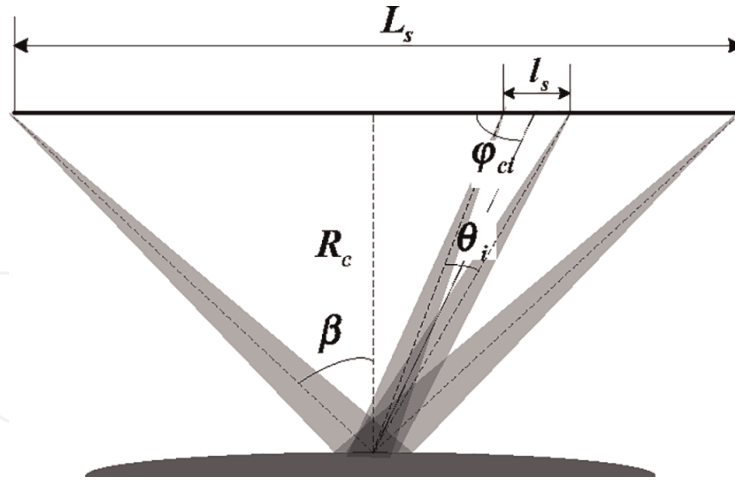
Figure 4.
The image geometrical mode of spaceborne video SAR.

The Doppler bandwidth of the ith video frame can be presented as follows.

$$Ba_i = fd_b - fd_a \approx \frac{2v_r \theta_i \sin \varphi_{ci}}{\lambda} \tag{4}$$

The azimuth resolution can be expressed as follows.

$$\rho_{ai} = \frac{v_g}{Ba_i} = \frac{\lambda v_g}{2v_r \theta_i \sin \varphi_{ci}} \tag{5}$$

Then the distance the radar moves of the ith video frame can be derived as follows.

$$L_i = \frac{\lambda v_g R_0}{2v_r \rho_{ai} \sin^3 \varphi_{ci}} = \frac{\lambda v_g \left(R_0^2 + v_r^2 t_i^2\right)^{3/2}}{2v_r \rho_{ai} R_0^2} \tag{6}$$

Where t_i is the middle time of the ith video frame.

In video SAR the synthetic aperture time to achieve the desired azimuth resolution typically exceed the frame period. As a result, there can be a significant overlap in the collected phase history used to form consecutive images in the video. **Figure 5**
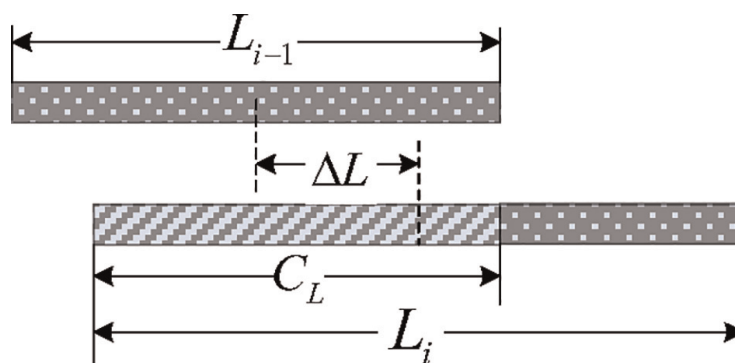

Figure 5.
The overlap between adjacent frames of video SAR.

illustrates the overlap between adjacent frames of video SAR, where L_i is the synthetic aperture length of the ith video frame, C_L is the overlap length of the adjacent frames. ΔL is the distance between adjacent frames.

The overlap length of the adjacent frames can be presented as follows.

$$C_{\mathrm{L}} = \frac{L_i}{2} + \left(\frac{L_{i-1}}{2} - \Delta L\right) = \frac{(L_i + L_{i-1})}{2} - \Delta L \tag{7}$$

Then the overlap rate can be expressed as follows.

$$\alpha_i = \frac{1}{2} + \frac{\lambda v_{\mathrm{g}}\left(R_0^2 + v_{\mathrm{r}}^2(t_i - T_{\mathrm{f}})^2\right)^{3/2} - 2T_{\mathrm{f}}v_{\mathrm{r}}^2 R_0^2 \rho_{ai}}{2\lambda v_{\mathrm{g}}\left(R_0^2 + v_{\mathrm{r}}^2 t_i^2\right)^{3/2}} \tag{8}$$

3.2 Spaceborne video SAR imaging based on BP algorithm

In the spaceborne video SAR system, the low-orbit satellite works in the spotlight mode, the video imaging is realized through the reasonable segmentation of the echo data, and the key technical problems to be solved in the spaceborne video SAR imaging mainly include as follows [19–26].

1. Large squint angle problem of some data frames

Since the LEO satellite works in the spotlight mode, some data frames have large squint angles, and there are serious range-azimuth coupling and range cell migration, which will lead to serious degradation of image quality by the traditional approximation method.

2. Data overlap of adjacent video frames

From the above analysis, it can be seen that in the spaceborne video SAR, since the synthetic aperture time is larger than the frame period, there is a large overlap of data between adjacent frames, and processing each frame individually will lead to repeated operations of overlapping data between adjacent frames, which will greatly reduce the operation efficiency.

3. Real-time problem

The spaceborne video SAR imaging needs to provide real-time or quasi-real-time video frame images, which requires the algorithm to have high computing efficiency, and the possibility of parallel computing needs to be explored based on the application of advanced computing hardware equipment.

A fast BP (Back-Projection) algorithm, which can be implemented in parallel, is proposed to address the imaging characteristics of space-based video SAR and the key technical problems to be solved. As an accurate time-domain algorithm, the BP algorithm avoids the geometric approximation, so it can well solve the problems of imaging under a complex distance model and the serious coupling between range and azimuth direction in the case of large squint angle in spaceborne video SAR [27].

In the application of the BP algorithm, the azimuth resolution increases with the increase of coherent cumulative pulse number, so the spaceborne video SAR imaging based on the BP algorithm can effectively avoid the repetitive operation of overlapping data of adjacent frames. The current frame can be imaged with the operation result of overlapping data of the previous frame, thus effectively improving the operation efficiency. At the same time, the sub-aperture division can further improve the operation speed of the BP algorithm, and the sub-aperture based processing can also realize parallel computing, which can effectively ensure the real-time or quasi-real-time output of video SAR images.

The process of spaceborne video SAR imaging based on the BP algorithm is shown in **Figure 6**, firstly, the echo signal is divided into several sub-apertures, and in order to achieve avoiding repeated operations through sub-aperture superposition, the frame period is required to be an integer multiple of the sub-aperture length, if the synthetic aperture length of a single video frame is L, and it is divided into N sub-apertures, the length of each sub-aperture is $L_{sub} = L/N$. The imaging of each sub-aperture can be calculated in parallel to the image of each sub-aperture can be computed in parallel to generate a low-resolution image, and finally, the full-resolution image of a single frame can be obtained by sub-aperture synthesis.

The range pulse compression signal in a single sub-aperture is as follows.

$$s_{BM(ij)}(\tau, \eta) = s_{B0(ij)}(\tau, \eta) \otimes s_{B0(ij)}^*\left[\left(T_{c(ij)} - \tau\right), \eta\right] \tag{9}$$

Where τ is the range time, η is the azimuth time, $T_{c(ij)}$ is the time delay of the reference point, since the echo time delay is difficult to coincide with the sampling point, the distance to the pulse compressed signal should be interpolated, and the interpolated signal is as follows.

$$S_{BUM(ij)}(t, \eta) = \sum_{|t-n\Delta\tau| \leq N_s} s_{BM(ij)}(n\Delta\tau, \eta) h_w(t - n\Delta\tau) \tag{10}$$

Where $\tau = n\Delta\tau$ is the sampling point before interpolation, $2N_s$ is the length of interpolation kernel, $h_w(t)$ is the interpolation kernel function after window sharpening. Since the processed echo data has been demodulated, the echo phase compensation is needed to achieve coherent accumulation, and the result after the echo phase compensation is as follows.

$$S_{BCUM(ij)}(t, \eta) = S_{BUM(ij)}(t, \eta) \exp\left(j2\pi f_c t\right) \tag{11}$$
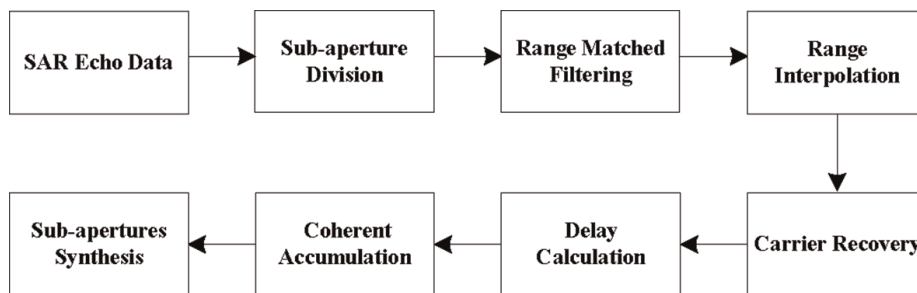

Figure 6.
Flow diagram of one frame SAR image formation.

The time delay between the target point and each radar position within the sub-aperture is as follows.

$$t_{ij}(n\Delta\eta) = R_{\mathrm{bi}(ij)}(n\Delta\eta)/c \qquad (12)$$

Where $\eta = n\Delta\eta$ is the azimuth sampling point, then the imaging result of the target P_{ij} in the *kth* sub-aperture is as follows.

$$f_{\mathrm{B}(ij)}^{k}(\alpha_i, \delta_j) = \sum_{n=R}^{S} S_{\mathrm{BCUM}(ij)}\left[t_{ij}(n\Delta\eta), n\Delta\eta\right] \qquad (13)$$

Where $R\Delta\eta$ is the starting time of the *kth* sub-aperture echo data, and $S\Delta\eta$ is the end time of the *kth* sub-aperture echo data, At this point, the low-resolution imaging result for the *kth* sub-aperture $f_{\mathrm{B}}^{k}(\alpha, \delta)$ is obtained by traversing each grid in the scene.

In the imaging process, the sub-apertures are calculated in parallel, which can effectively improve the computing efficiency. Finally, the low-resolution images of sub-apertures are coherently added to obtain the full-resolution image of the *ith* video frame as follows.

$$F_i(\alpha, \delta) = \sum_{k=1}^{N} f_{\mathrm{B}}^{k}(\alpha, \delta) \qquad (14)$$

3.3 Simulation

To validate the video SAR algorithm, a point target simulation is carried out based on the parameters in **Table 1**.

The scene size is $2 \times 2\,\mathrm{km}$. There are 25 point targets in the simulated scene, the initial moment is arranged uniformly by 5×5, the first and fifth columns and the first and fifth rows of the point targets are stationary, and the coordinates of the target in the center of the scene are assumed to be $(0, 0)$. The motion parameters of the remaining targets are shown in **Table 2**.

Parameters	Values
Earth Radius (km)	6378
Orbital Eccentricity	0
Orbital Inclination (°)	20
Orbital Height (km)	567
Longitude of Ascending Node (°)	300
Radar Center Frequency (GHz)	9.6
Transmitted Pulse Duration (us)	30
Transmitted Signal Bandwidth (MHz)	150
Azimuth Resolution (m)	1
Video Frame Rate (Hz)	5

Table 1.
Parameters for simulation.

目标	坐标	$v_r/(\text{km·h}^{-1})$	$a_r/(\text{km·h}^{-2})$	$v_a/(\text{km·h}^{-1})$	$a_a/(\text{km·h}^{-2})$
$S(2,2)$	$(-0.5, 0.5)$	-15	0	0	0
$S(2,3)$	$(0, 0.5)$	-10	0	0	0
$S(2,4)$	$(0.5, 0.5)$	0	0	0	50
$S(3,2)$	$(-0.5, 0)$	0	0	120	0
$S(3,3)$	$(0, 0)$	0	0	200	0
$S(3,4)$	$(0.5, 0)$	0	-5	0	0
$S(4,2)$	$(-0.5, -0.5)$	15	0	120	0
$S(4,3)$	$(0, -0.5)$	10	0	200	0
$S(4,4)$	$(0.5, -0.5)$	0	-5	0	50

Table 2.
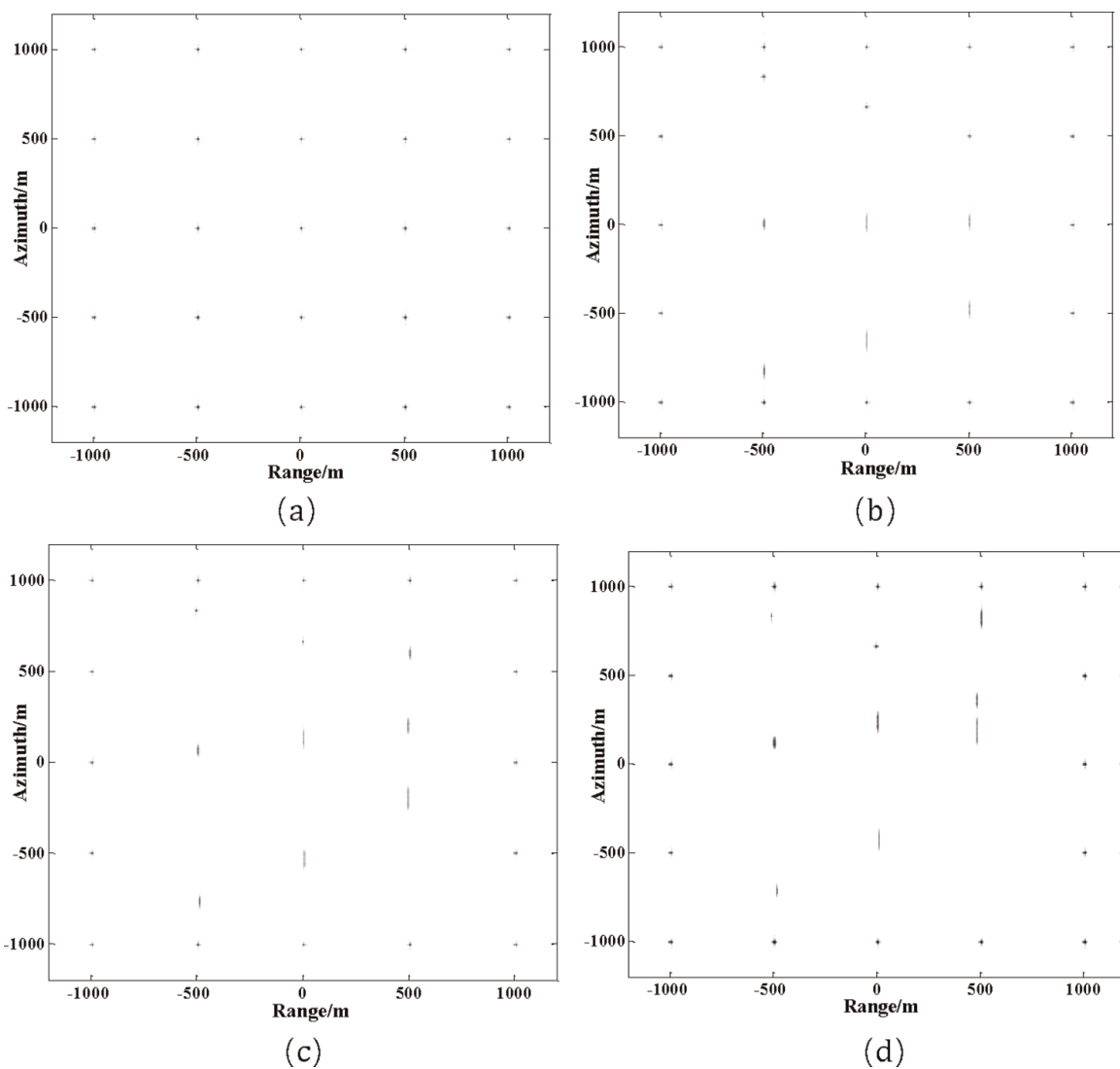*Motion parameters of moving targets.*

Figure 7.
Image formation result of spaceborne video SAR. (a) Stationary target imaging results (b) The first frame of the video SAR (c) The 10th frame of the video SAR (d) The 18th frame of the video SAR.

The results of spaceborne video SAR simulation are shown in **Figure 7** with a frame rate of 5 Hz, where **Figure 7(a)** shows the imaging results of 25 points when the target is stationary in the initial state, and it can be seen that the target achieves a good focusing effect at each point when the target is stationary. **Figure 7(b)** shows the imaging results of the 1st frame of the spaceborne video SAR, and the comparison of the imaging results of $S(2, 2)$, $S(2, 3)$ and $S(2, 4)$ show that the larger the velocity in the range direction, the larger the offset of the azimuth direction of the target, and the velocity in the range direction and the acceleration in the azimuth direction have less influence on the azimuth spreading of the target. The comparison of the imaging results of $S(3, 2)$, $S(3, 3)$ and $S(3, 4)$ show that the larger the azimuth velocity of the target, the more serious the azimuth spread of the target, and the range acceleration is also the main cause of the azimuth spread of the target. From the imaging results of $S(4, 2)$, $S(4, 3)$ and $S(4, 4)$, it can be seen that when the target has both azimuth velocity, range velocity and range acceleration, the azimuth image of the target is both shifted and defocused. **Figure 7(c)** and **(d)** show the imaging results of frame 10 and frame 18 of the spaceborne video SAR respectively. From the imaging results of $S(2, 4)$, $S(3, 4)$ and $S(4, 4)$, it can be seen that the azimuth velocity and range velocity of the three targets gradually become larger and the azimuth spreading and shifting become larger as the time increases. It can be seen that the imaging results of spaceborne video SAR correctly reflect the motion information of the targets, which can provide the basis for the subsequent motion target detection, motion parameter estimation and repositioning and imaging of the moving targets based on SAR video.

4. Conclusions

In this chapter, a general definition of spaceborne video SAR is given first, and three operating modes and possible application directions of spaceborne video SAR are proposed for the demand of long-time observation. The imaging duration of spaceborne video SAR is mainly affected by the incidence angle, azimuth sweeping capability and the maximum squint angle allowed by the imaging process. The analysis shows that for low-orbit satellites, the angle of incidence is the main factor limiting the duration of video SAR. Then a parallel computable video SAR imaging algorithm based on sub-aperture division is proposed for the three types of key technical problems to be solved in spaceborne video SAR imaging, and computer simulation is conducted to verify the results. The simulation results show that the video imaging results correctly reflect the motion of the target and can provide the basis for the motion target detection, parameter estimation, and repositioning and imaging based on SAR video. The research results of this chapter can provide suggestions and references for the construction and application of future spaceborne video SAR systems.

Conflict of interest

The authors declare no conflict of interest.

Author details

Jian Liang* and Liang An
Institute of Remote Sensing Satellite, China Academy of Space Technology, Beijing,
China

*Address all correspondence to: liangjiancast@163.com

IntechOpen

References

[1] DARPA. Video synthetic aperture radar (ViSAR). Broad Agency Announcement. 2012:DARPA-BAA-12-41:1-51

[2] Well L, Doerry A, et al. Developments in SAR and IFSAR System and Technologies at Sandia National Laboratories. Vol. 2. Big Sky, MT, USA: IEEE; 2005. pp. 1085-1095

[3] Available from: http://www.sandia.gov/radar

[4] Damini A, Balaji B, Parry C. A video SAR mode for the X-band wideband experimental airborne radar. Proceedings of SPIE. 2010;**7699**(0E):1-11

[5] Moses RL, Joshua N. Recursive SAR imaging. In: Proceedings of the SPIE Algorithms for Synthetic Aperture Radar Imagery XV. Orlando, FL, USA: Ohio State University Department of Electrical and Computer Engineering Columbus OH USA. Vol. 6970. 2008. pp. 1-12

[6] Defense Advanced Research Projects Agency. Broad Agency Announcement: Video Synthetic Aperture Radar System Design And Development. DARPA, USA: Arlington; 2012

[7] Wallace HB. Development of a video SAR for FMV through clouds. Proceedings of SPIE. 2015;**9479**(0L):1-2

[8] Palma S, Wahlen A, Stanko S, et al. Real-time onboard processing and ground based monitoring of FMCW-SAR videos. In: The 2014 EUSAR. Vol. 3607. Berlin: IEEE; 2014. pp. 2-5

[9] Cumming IG, Wong FH. Digital Processing of Synthetic Aperture Radar Data Algorithms and Implementation. London: Artech House Inc; 2005

[10] Curlander JC, McDonough RN. Synthetic Aperture Radar: Systems and Signal Processing. NY, USA: John Wiley and Sons, Inc.; 1991

[11] Elachi C. Spaceborne Radar Remote Sensing: Applications and Techniques. New York: The Institute of Electrical and Electronic Engineers, Inc; 1987:33-42

[12] Damini A, Mantle V, Davidson G. A new approach to coherent change detection in video SAR imagery using stack averaged coherence. In: The 2013 IEEE Radar Conference. Vol. 5794. Ottawa, ON, Canada: IEEE; 2013. pp. 13-17

[13] Carrara WG, Goodman RS, Majewski RM. Spotlight Synthetic Aperture Radar: Signal and Processing Algorithms. Norwood, MA, USA: Artech House; 1995

[14] Kirscht M. Detection and velocity estimation of moving objects in a sequence of single-look SAR images. Physical Review A. 1996;**1**(5):333-335

[15] Ouchi K. On the multi look images of moving targets by synthetic aperture radars. IEEE Transactions on Antennas and Propagation. 1985;**8**(33):823-827. DOI: 10.1109/TAP.1985.1143684

[16] Kirscht. Method of detecting moving objects and estimating their velocity and position in SAR images United States Patent, 2005.10.04:US6952178B2

[17] Kirscht M. Detection and imaging of arbitrarily moving targets with single-channel SAR. Radar, Sonar and Navigation, IEEE Proceedings. 2003;**150**(1):7-11. DOI: 10.1109/RADAR.2002.1174697

[18] Yang J, Liu C, Wang Y. Imaging and parameter estimation of fast-moving targets with single-antenna SAR. IEEE Geoscience and Remote Sensing Letters. 2014;**11**(2):529-533. DOI: 10.1109/LGRS.2013.2271691

[19] Zhao S, Chen J, Yang W, et al. Image formation method for spaceborne video SAR. In: IEEE 5th Asia-Pacific Conference on Synthetic Aperture Rad. Singapore: IEEE; 2015. pp. 148-151

[20] Linnehan R, Miller J, Bishop E. An autofocus technique for video-SAR. Proceedings of SPIE. 2013;**8746**(08):1-10

[21] Miller J, Bishop E, Doerry A. Applying stereo SAR to remove height-dependent layover effects from video SAR imagery. Proceedings of SPIE. 2014; **9093**(3A):1-10

[22] Hawley RW, Garber WL. Aperture weighting technique for video synthetic aperture radar. Proceedings of SPIE. 2011;**8051**(07):1-7

[23] Jinping S, Zhifeng Y, Wenb H. A new subaperture chirp scaling algorithm for spaceborne spotlight SAR data focusing. In: The 2007 IEEE Radar Conference. Vol. 5794. London: IEEE; 2013. pp. 13-17

[24] Kaizhi Wang, Xingzhao Liu. Squint-spotlight SAR imaging by sub-band combination and rage-walk removal. Geoscience and Remote Sensing Symposium. Vol. 8742:(2) Alaska: IEEE; 2004. 3930-3933.

[25] Jin L, Liu X, Wang J. Adaptive subaperture approach for spotlight SAR azimuth processing. In: Geoscience and Remote Sensing Symposium. Boston: IEEE. Vol. 2808:(3) 2008: 1292-1295.

[26] Wang W, Ma X. A novel data preprocessing method for resolving doppler ambiguity of spaceborne spotlight SAR. In: Geoscience and Remote Sensing Symposium. Munich: IEEE; Vol. 978:(1) 2012:5-8.

[27] Miller J, Bishop E, Doerry A. An application of backprojection for Video SAR image formation exploiting a subaperture circular shift register. Proceedings of SPIE. 2013;**8746**(09):1-14